

RESEARCH

Open Access



# Mechanical Properties and Microstructure of Basalt Fiber Reinforced Concrete Under the Single-Side Salt-Freezing–Drying–Wetting Cycles

Hao Zeng<sup>1</sup>, Jin Zhang<sup>1,3\*</sup>, Yang Li<sup>1</sup>, Xin Su<sup>2</sup>, CongZhi Gu<sup>1</sup> and Kai Zhang<sup>1</sup>

## Abstract

In the past, the salt freezing test does not often accord with the actual service environment of engineering, thus, we designed a test method of single-side salt-freezing–drying–wetting cycles. The mechanical properties and microstructure of ordinary concrete and basalt fiber reinforced concrete were studied. The mechanical property test is aimed at the splitting tensile strength and compressive strength of concrete after different cycles. The microstructure test is to study the hydration products by scanning electron microscope (SEM) and the pore structure of concrete by mercury intrusion porosimetry (MIP) test. The results indicate that the addition of basalt fiber can improve the compactness and pore structure of concrete. It is beneficial to enhance the durability of concrete under single-side salt-freezing–drying–wetting cycles. The improving effect of basalt fiber is better on the splitting tensile strength of concrete than the compressive strength. Basalt fiber exerts the best effect on reducing harmful holes in concrete. However, there is an optimal range of basalt fiber content, the performance of concrete will deteriorate with excessive fiber content. The cycles will destroy the hydration products of concrete and the synergistic effect between hydration products and fibers, but has little effect on the three-dimensional network constructed by basalt fibers. The pore structure of concrete is correlated with the mechanical properties of it under cyclic conditions, which is worth further study.

## Highlights

1. Through the design of this single-side salt-freezing–drying–wetting cycle test method more truly reflects the impact of the service environment on concrete (ordinary concrete, basalt fiber reinforced concrete).
2. Through the comparative study of macroscopic mechanical properties and microstructure, the failure mechanism of concrete (ordinary concrete, basalt fiber reinforced concrete) and the main strengthening mechanism of basalt fiber under single-side salt-freezing–drying–wetting cycle were revealed.

Journal information: ISSN 1976-0485/eISSN 2234-1315

\*Correspondence: zhangjinzbst@hbut.edu.cn

<sup>3</sup> Department of Architectural Engineering, School of Civil, Architectural and Environmental Engineering, Hubei University of Technology, 28 Nanli Road, Wuhan 430068, People's Republic of China  
Full list of author information is available at the end of the article



© The Author(s) 2022. **Open Access** This article is licensed under a Creative Commons Attribution 4.0 International License, which permits use, sharing, adaptation, distribution and reproduction in any medium or format, as long as you give appropriate credit to the original author(s) and the source, provide a link to the Creative Commons licence, and indicate if changes were made. The images or other third party material in this article are included in the article's Creative Commons licence, unless indicated otherwise in a credit line to the material. If material is not included in the article's Creative Commons licence and your intended use is not permitted by statutory regulation or exceeds the permitted use, you will need to obtain permission directly from the copyright holder. To view a copy of this licence, visit <http://creativecommons.org/licenses/by/4.0/>.

3. The correlation calculation proves that the mechanical properties of concrete (ordinary concrete, basalt fiber reinforced concrete) are highly correlated with porosity, pore size distribution and critical pore size under single-side salt-freezing–drying–wetting cycle.
4. The sensitive aperture of compressive strength and splitting tensile strength of concrete (ordinary concrete, basalt fiber reinforced concrete) under single-side salt-freezing–drying–wetting cycle is calculated, which provides a reference for further comprehensive analysis and calculation.

**Keywords:** basalt fiber reinforced concrete, single-side salt-freezing–drying–wetting cycle, compressive strength, splitting tensile strength, pore structure

## 1 Introduction

In recent years, with the construction of large-scale infrastructure in various complicated service environments, higher demands are put forward for the mechanical and durability properties of concrete. At present, the application of fiber-reinforced technology to improve the performance of concrete has become one of the research hot spots in the field of building materials (Dhand et al., 2015; Khaled et al., 2011; Sukontasukkul et al., 2010). As a kind of high brittle material, ordinary concrete has disadvantages such as low splitting tensile strength and poor cracking resistance (Kayali et al., 2003; Rashiddadash et al., 2014), which brings some troubles to many engineering applications. Adding fiber to concrete can improve the brittleness of concrete and to improve the strength and durability of concrete (Afroughsabet & Ozbakkaloglu, 2015; Kuder & Shah, 2010; Lau & Anson, 2006; Yang et al., 2019; Yao et al., 2019). Made of natural basalt ore as raw material through hot melting and wire drawing at high temperature (Gzigany et al., 2005; Sim et al., 2005), basalt fiber is a new type of inorganic fiber possessing a series of advantages of high strength, excellent size stability, insulation and heat insulation, strong corrosion resistance, easy processing, low price and high compatibility (Flore et al., 2015; Wang et al., 2013; Yew et al., 2015). Compared with those of metal fiber, the insulation performance and corrosion resistance of basalt fiber make it more suitable for road and high-speed railway engineering. Basalt fiber is also an environmental-friendly material (Krasnovskih et al., 2014; Ludovico et al., 2012), the application of which in the field of concrete will meet the two requirements of green and sustainable development of concrete and concrete modification at the same time, which has great research value.

After studying the basic properties of carbon fiber, glass fiber and basalt fiber based on concrete, Sim and Park (2005) found that basalt fiber concrete had better performance than carbon fiber concrete and glass fiber concrete. Basalt fiber can improve engineering mechanics and durability. The experimental results of Kizilkanat et al. (2015) showed that the splitting tensile strength of

basalt fiber concrete would increase with the increase of fiber content. The mechanical test results of Afroz et al. (2017) also showed that even after 56 days, the modified basalt fiber could still significantly improve the splitting tensile strength and flexural strength of concrete. Zeynep and Mustafa (2018) studied the influence of basalt fiber of different lengths on the mechanical properties of self-compacting concrete, and the results indicated that the compressive strength of concrete would be the highest when the volume content of basalt fiber was 0.1% and the length was 12 mm. When the volume content is 0.5% and the length is 24 mm, the splitting tensile strength will be the highest. Branston et al. (2016) studied the application of short-cut basalt fiber in concrete. Among the basalt fiber with the same quality content, the compressive strength of 50-mm basalt fiber concrete is higher than that of 36-mm basalt fiber concrete. Basalt fiber content over 12 kg/m<sup>3</sup> will lead to fiber aggregation. Dias and Thaumaturgo (2005) believe that basalt fiber can substantially enhance the mechanical properties of concrete when the fiber volume content is of 0.5%, and it can also significantly reduce the early shrinkage of concrete and improve the early performance of concrete. Khan et al. (2018) studied the influence of different content of basalt fiber on the mechanical properties of concrete, through the stress–strain curve and load–deflection curve of which, it is found that the mechanical properties of basalt fiber concrete decreased significantly when the content of basalt fiber exceeded 0.68%. By adding chopped basalt fiber into concrete, High et al. (2015) studied the change of bending resistance and found that the bending resistance of concrete could be significantly promoted. In research of Li and Wu (2009), basalt fiber has a certain improvement in deformation ability of geopolymer concrete. Sadrmomtazi et al. (2018) studied the influence of silica fume on the mechanical properties of basalt fiber reinforced cement-based composites, and the results showed that the working performance of concrete would decrease with the increase of fiber content. When the fiber content was 1.5% and silica fume content was 15%, the fiber in concrete would

appear agglomeration. The flexural strength of concrete increased while the compressive strength decreased with the addition of fiber, while the flexural strength increased twice with the addition of fiber and silica fume. The study of Zhang et al. (2017) shows that the interface adhesion between basalt fiber and concrete is high, but the adhesion between cement base and aggregate cannot be improved, and basalt fiber has a good crack resistance effect on concrete. Adding basalt fiber into shotcrete can significantly augment the mechanical properties and working performance of basalt fiber shotcrete (BFRC) as well as the microstructure of shotcrete, and effectively suppress the deformation of roadway surrounding rock (Bernard, 2015; Dong et al., 2017; Khooshechin & Tanzadeh, 2018). The basalt fiber mixing in concrete formed irregular three-dimensional network, which is closely connected with cement paste and aggregate. Doped fiber can decrease the porosity to a certain extent, delay the development of the internal microscopic cracks, and concrete more compact structure (Monaldo et al., 2019). Jiao et al. (2019) showed that basalt fiber reduced the number of macropores through NMR studies. To explore basalt fiber concrete's ability to resist impact load, Elmahay and Verleysen (2019) studied the basalt fiber reinforced concrete under high strain rate effect of tensile properties, finding that basalt fiber reinforced concrete in the filling direction and bending direction are sensitive to strain rate, whose material stiffness, Poisson's ratio and ultimate tensile strength and ultimate tensile strain increases with the increase of strain rate. With the application of SEM, it was found that the fracture morphology was independent of strain rate, and there were stratification phenomena at all strain rates. Compared with ordinary concrete, basalt fiber concrete exhibited excellent energy absorption capacity at high strain rate, which makes it a good candidate material for impact resistance construction. Through the investigation of the dynamic characteristics of basalt fiber reinforced concrete under high temperature, Ren et al. (2016) found that the dynamic strength, critical strain and impact toughness of basalt fiber reinforced concrete at different temperatures achieved a positive correlation with dynamic load rate, showing obvious rate sensitivity. Zhao et al. (2018) observed the internal loss process of concrete under freezing–thawing conditions, whose results showed that basalt fiber could inhibit the internal damage and failure of concrete, however, it had little relation with the content of fiber. Shengji et al. (2015) has conducted an experimental study on the durability of basalt fiber reinforced concrete in engineering application. It is concluded that basalt fiber has a significant effect on enhancing the freezing–thawing damage resistance of concrete under corrosion conditions. Aybu et al. (2014) believed that basalt fiber could

significantly improve the chloride ion permeability resistance of concrete, whereas some scholars held opposing views (Huang et al., 2015). Taha et al. (2020) found that basalt fiber reinforced concrete (BFRC) has higher bonding strength with steel bar in saline–alkali environment and higher reliability in bonding slip test. Lee et al., (2014) studied the chemical stability of basalt fiber in alkaline solution, finding that basalt fiber soaked in weak alkaline solution will be very stable, the mass loss rate of which is low after soaking in  $\text{Ca}(\text{OH})_2$  solution for 3 months. The compressive strength of early-age concrete in corrosion solution is negatively correlated with the content of basalt fiber (Lu et al., 2017). Gao et al. (2013) studied the corrosion process of sulfate on concrete under bending load and dry–wet cycle, indicating that stress level has greatly influenced the concrete durability. Bassuoni and Nehdi (2009) studied the sulfate resistance of concrete under dry–wet cycles and bending loads. It is denoted by the results that the mechanism of concrete erosion is different from that of a single failure mechanism (sulfate erosion) under combined action. Sahmaran et al. (2007) carried out an experimental study on the long-term properties of concrete under the dry–wet cycle sulfate erosion, the results of which showed that, compared with the total sulfate immersion environment, the damage degradation rate of mechanical properties of concrete under the dry–wet cycle erosion increased significantly.

At present, studies on the influence of basalt fiber on concrete properties are mainly focused on the influence of basalt fiber on concrete mechanical properties, or the durability of concrete in a single environment, but durability studies under the coupling effect of multiple environments relatively in deficiency. In northeast and northwest China, many construction projects are geographically faced with the cold environment for a long time, during which concrete structures will be damaged by freezing–thawing under the condition of low temperature and high cold, which seriously threatens the long-term safe use of building structures and brings huge economic and property losses along with huge repair costs. The structures in service in some specific environments, such as roads in industrial factories and sewage pipeline systems, face the coupling effects of freezing–thawing cycle (mostly frozen on single side), sulfate erosion, drying–wetting cycle and so on. The drying–wetting cycle accelerates sulfate erosion, causing more obvious durability loss of concrete (Bassuoni & Nehdi, 2009; Gao et al., 2013). Therefore, the study of the mechanics and durability of basalt fiber reinforced concrete under the complex coupling action of single-side salt-freezing–drying–wetting cycle is of positive practical significance for improving the service stability of such structures, yet currently, this kind of research

**Table 1** Main chemical composition of cement (%)

Materials	CaO	SiO <sub>2</sub>	Al <sub>2</sub> O <sub>3</sub>	Fe <sub>2</sub> O <sub>3</sub>	MgO	SO <sub>3</sub>	MnO	Other
Cement	65.37	21.22	2.53	3.09	2.39	1.91	–	3.49

**Fig. 1** Basalt fiber.

has not been reported. According to the actual service environment of this kind of structure, we designed an experimental method of single-side salt-freezing–drying–wetting cycle, and carried out the research on the mechanical properties and mesostructure of basalt fiber reinforced concrete with different volume content under the single-side salt-freezing–drying–wetting cycle. This paper mainly studied the influence of single-side salt-freezing–drying–wetting cycle on compressive

strength and splitting strength of basalt fiber reinforced concrete, exploring the pore structure, basalt fiber morphology and hydration product changes by MIP (mercury intrusion porosimetry) test and SEM (scanning electron microscopy) test, and explored the damage reason from the microscopic structure.

## 2 Experimental

### 2.1 Raw Materials

**Cement:** PO42.5 Portland cement produced by Wuhan Huaxin Cement Company, possessing a specific surface area of 360 m<sup>2</sup>/kg and a density of 3.15 g/cm<sup>3</sup>. (See Table 1 for the main chemical composition of cement.) **Basalt fiber (Fig. 1):** produced by a company in Guangdong (see Table 2 for basic performance and size of basalt fiber). **Coarse aggregate:** continuous graded granite gravel, particle size 5–20 mm. **Fine aggregate:** native river sand, particle size 0–4.75 mm. **Water:** laboratory tap water. **Water reducing agent:** naphthalene series efficient water reducing agent, whose water reduction rate is of more than 20%. A total of four experimental groups were set, with 30 specimens in each group. Group C was pure cement concrete, and BFRC1, BFRC2, BFRC3 was basalt fiber reinforced concrete (basalt fiber content by volume was 0.1%, 0.2%, 0.3%, respectively). Concrete design strength grade is C40 (see Table 3 for specific mix ratio).

**Table 2** Physical and mechanical properties of basalt fibers.

Length (mm)	Diameter (μm)	Density (kg/m <sup>3</sup> )	Fracture ductility rate (%)	Elastic modulus (GPa)	Tensile strength (MPa)	Moisture content (%)
28	14	2750	2.5–3.1	90–110	3000–4500	0.060

**Table 3** Mix proportions.

Symbol	W (C)	W (kg/m <sup>3</sup> )	C (kg/m <sup>3</sup> )	BF (vol%)	S (kg/m <sup>3</sup> )	A (kg/m <sup>3</sup> )	Ads (kg/m <sup>3</sup> )
C	0.4	185	462	0.00	635	1178	3
BFRC1	0.4	185	462	0.01	635	1178	3
BFRC2	0.4	185	462	0.02	635	1178	3
BFRC3	0.4	185	462	0.03	635	1178	3

W water, C cement, BF basalt fiber, S fine aggregate, A coarse aggregate, Ads water reducing agent.



**Fig. 2** The single-side salt-freezing–drying–wetting cycle tests.

cycles), soaking for 8 h, and drying at 65 °C oven for 8 h, making the total cycle time 32 h. The freezing–thawing and soaking medium was 5% sodium sulfate solution, and the depth of the solution was kept 5 mm from the frozen surface to the liquid surface of the specimen. To ensure the stability of the solution concentration, the solution was replaced every 10 times. A total of 5, 10, 15, 20 times of single-side salt-freezing–drying–wetting cycle tests were set up. Schematic diagram of specimen and device is shown in Figs. 2, 3).

- (2) Mechanical properties test (Fig. 4): the compressive strength and splitting tensile strength were tested, respectively, after standard curing for 28 days; after 5, 10, 15 and 20 times of single-side salt-freezing–drying–wetting cycle, the compressive strength and splitting tensile strength of the specimens were

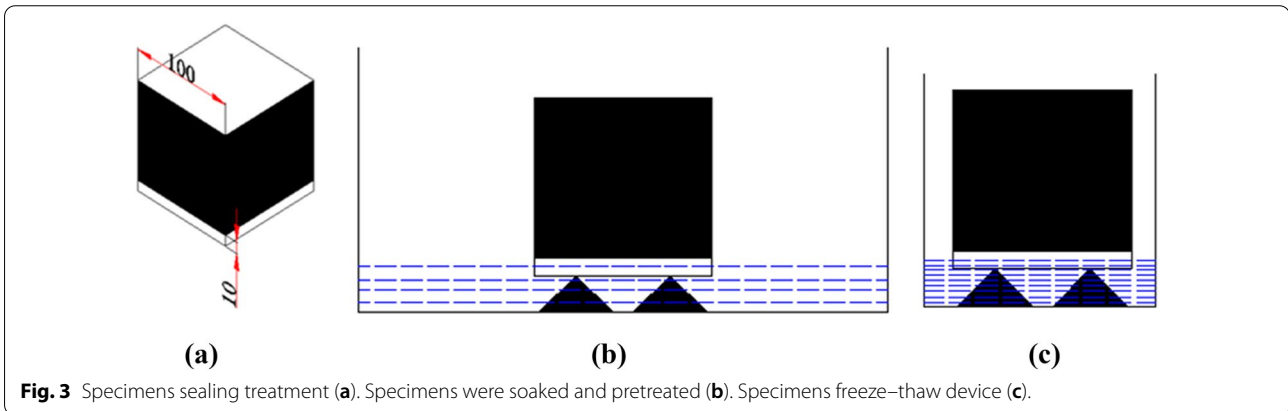


**Fig. 3** Specimens sealing treatment (a). Specimens were soaked and pretreated (b). Specimens freeze–thaw device (c).

## 2.2 Experimental Scheme

- (1) Single-side salt-freezing–drying–wetting cycle test: For single-side freezing–thawing test, refer to the “single-side freezing–thawing method” specified in GB/T 50081-2009. The cube specimen of 100 mm × 100 mm × 100 mm after 28 days of standard curing was used, the top surface opposite to the frozen surface was reserved, and the remaining four sides were sealed with epoxy resin (10-mm blank space was reserved from the frozen surface). After the epoxy resin glue is dried, the treated specimen is placed in a plastic container, the bottom of which is supported with 5-mm-thick gasket. Then 5% sodium sulfate solution is injected into the specimen and the distance from the frozen surface to the liquid surface should be 5 mm. The pretreatment soaking time is 3 days. Single-side salt-freezing–drying–wetting cycle test consists of single-side salt freezing–thawing cycle of 16 h (a freezing–thawing cycle of 4 h, total of 4 times of freezing–thawing



**Fig. 4** Mechanical testing machine.

tested, respectively (the frozen surface was taken as the bearing surface). The value of three specimens in each group was taken on average.

- (3) SEM test: the mortar blocks were broken on the concrete surface after standard curing for 28 days. The mortar blocks were broken on the frozen surface after single-side salt-freezing–dry–wet cycle (20 times), which were dried for 24 h in a 65 °C oven for SEM test.
- (4) MIP test: the mortar blocks were broken on the concrete surface after standard curing for 28 days, and the mortar blocks were broken on the frozen surface after single-side salt-freezing–dry–wet cycle (5 times, 10 times, 15 times, 20 times), and the hydration was suspended with anhydrous ethanol, and the MIP test was carried out after dried for 48 h in the oven at 65 °C.

### 3 Results and Discussion

#### 3.1 Mechanical Properties

As can be seen from Fig. 5, the addition of basalt fiber improves the initial compressive strength of concrete, and the initial compressive strength of BFRC1, BFRC2 and BFRC3 groups increases by 8.2%, 11.8% and 3.9%, respectively, compared with group C. The incorporation of basalt fiber elevates the compactness and cohesiveness of hydration products of concrete, reduces the defects caused by early shrinkage of concrete, and contributes to the improvement of concrete strength (Dias & Thaumaturgo, 2005; Monaldo et al., 2019). Excessive incorporation of basalt fiber, however, will increase the

disorderly distribution of fiber on the one hand, resulting in fiber agglomeration (Branston et al., 2016), where the defect rate of concrete will be increased as well. The excessive incorporation of basalt fiber reduces the content of concrete cementitious material per unit volume, as a result, the positive effect of BFRC3 group is inferior to those of BFRC1 and BFRC2 groups. It can also be seen (Fig. 6) from the mechanical experiment of 0 cycles that the addition of basalt fiber improves the failure mode of concrete specimens, meanwhile, the cracks of basalt fiber concrete specimens are reduced compared with ordinary concrete. Even under stress, the integrity of basalt fiber concrete specimens is still higher. Under single-side salt-freezing–drying–wetting cycle, the compressive strength of concrete begins to decrease with the increase of cycle times. After 5 cycles, the loss rate of compressive strength in group C, BFRC1, BFRC2 and BFRC3 were 2.4%, 1.2%, 0.6% and 1.1%, respectively. After 10 cycles, the loss rates of compressive strength in group C, BFRC1, BFRC2 and BFRC3 were 8.0%, 4.1%, 3.6% and 7.5%, respectively. After 15 cycles, the loss rates of compressive strength in group C, BFRC1, BFRC2 and BFRC3 were 21.3%, 11.3%, 6.9% and 15.4%, respectively. After 20 cycles, the loss rates of compressive strength in group C, BFRC1, BFRC2 and BFRC3 were 33.9%, 24.6%, 15.5% and 27.3%, respectively. The compressive strength loss rate of basalt fiber reinforced concrete in each group is lower than that of ordinary concrete under single-side salt-freezing–drying–wetting cycle. On the one hand, the addition of basalt fiber improves the compactness of concrete and reduces the erosion content and depth of sulfate ion; on the other hand, the three-dimensional network constructed by basalt fibers and the high elastic modulus of it can offset part of the tensile stress caused by icing pressure (Musa & Yang, 2006), capillary osmotic pressure (Powers, 1954) and the expansion stress caused by sulfate crystallization in the single-side salt-freezing–drying–wetting cycle.

In terms of splitting tensile strength (Fig. 7), compared with that of group C, the initial strength of BFRC1, BFRC2 and BFRC3 groups increased by 11.5%, 17.3% and 28.8%, respectively. The improvement rate of BFRC3 group was the highest, which was different from the factor of compressive strength. The addition of basalt fiber played its reinforcing and toughening role, and the higher the fiber content, the more obvious the effect. After 5 cycles, the loss rates of splitting tensile strength in group C, BFRC1, BFRC2 and BFRC3 were 7.8%, 3.4%, 1.6% and 1.5%, respectively. After 10 cycles, the loss rates of splitting tensile strength in group C, BFRC1, BFRC2 and BFRC3 were 17.3%, 8.6%, 3.3% and 9.0%, respectively. After 15 cycles, the loss rates of splitting tensile strength in group C, BFRC1, BFRC2 and BFRC3 were 23.1%,

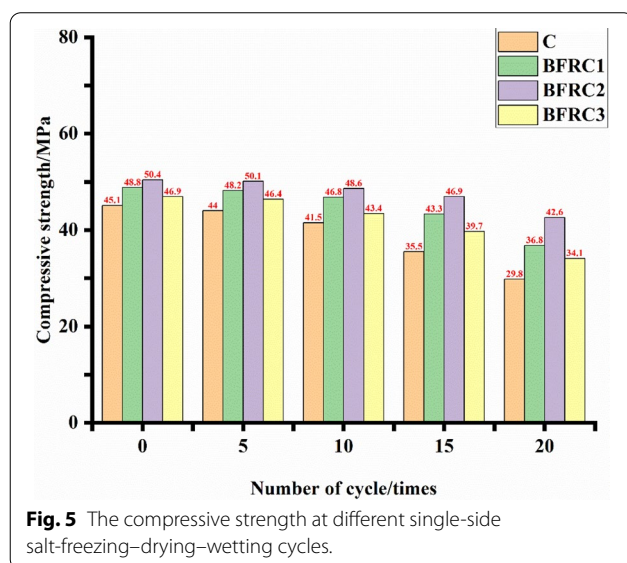




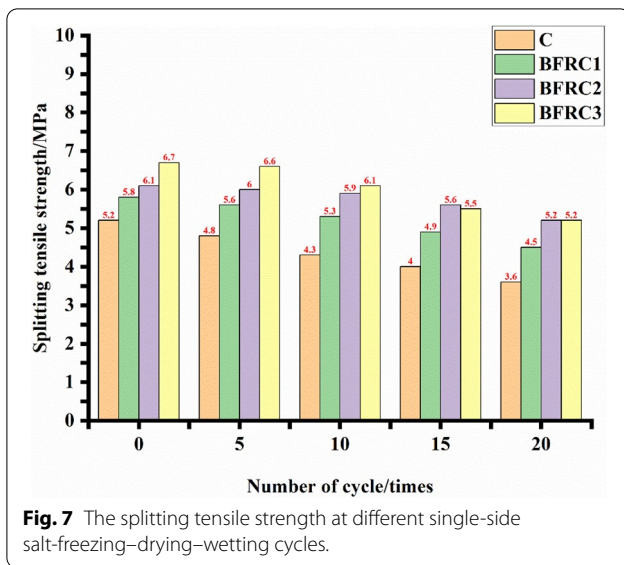
**Fig. 6** Concrete compression failure pattern.

15.5%, 8.2% and 19.7%, respectively. After 20 cycles, the loss rates of splitting tensile strength in group C, BFRC1, BFRC2 and BFRC3 were 30.8%, 22.4%, 14.8% and 22.4%, respectively. It can be concluded that basalt fiber under single-side salt-freezing–drying–wetting cycle environment also has a positive effect of reducing the concrete splitting tensile strength loss rate. And the single-side salt-freezing–drying–wetting cycle has little effect on basalt fiber and its three-dimensional network, so after 20 cycles, basalt fiber reinforced concrete splitting tensile strength loss rate is lower than the compressive strength loss rate. Although the splitting tensile loss rate of BFRC3 group was greater than that of BFRC1 and BFRC2 groups,

the splitting tensile strength of BFRC3 group and BFRC2 group were 5.2 MPa after 20 cycles, which was better than that of BFRC1 group.

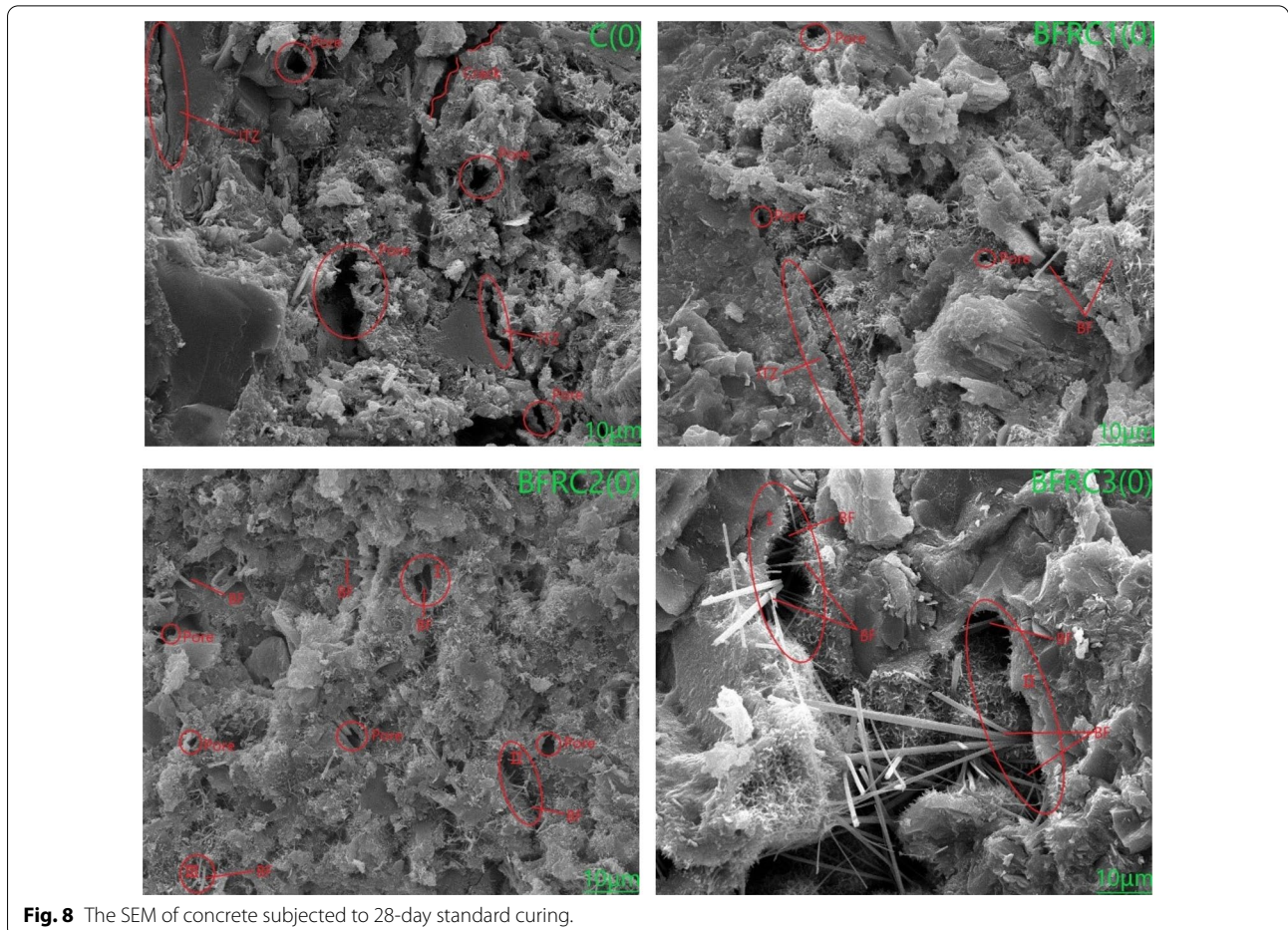
### 3.2 Microstructure

Hydration process of Portland cement is a complex chemical reaction, the hydration products of which include calcium hydroxide crystal, C–S–H gel, ettringite and so on. Among them, C–S–H gel is the main product of hydration of Portland cement. In the fully hydrated cement slurry, C–S–H gel accounts for about 70%, which is principally due to the strength of cement. Various hydration products are related to each other to form a



spatial network, and the shape of the spatial network has an important role to play in the performance of concrete. ITZ area refers to the interface transition area between coarse and fine aggregate and cement slurry in concrete. With the high porosity and the low hardness, ITZ area contains a lot of hydration product CH (calcium hydroxide crystal) of low density, consequently, the mechanical properties of ITZ are worse than the physical properties of cement mortar, making it the weak link of cement-based composites (Ollivier et al., 1995).

As can be seen from Fig. 8-C(0), hydration products of ordinary concrete are randomly distributed. Pores, micro-cracks and other defects can be clearly observed in the interface, where some hydration products are not closely connected. In the two marked ITZ areas, we can see that there are obvious cracks at the bond between hydration products and aggregate, which are not closely connected. Compared with ordinary concrete, it can be seen in Fig. 8-BFRC1(0) and Fig. 8-BFRC2(0) that after the addition of basalt fiber, the interface pores of hydration products become smaller and no obvious micro-cracks are observed, which is beneficial to the



improvement of mechanical properties and durability of concrete. The natural compatibility of basalt fibers and cement-based composites are the main reasons for basalt fibers to blend and wrap with hydration products. However, due to the small fiber content, the ITZ area of BFRC1(0) is lower than that of BFRC2(0), yet still better than that of BFRC3(0). In BFRC2(0) region I, basalt fibers can be observed to cross the pores; in region II and III, basalt fibers can be observed to bridge the two ends of the ITZ areas, which greatly improves the tightness and stability of the ITZ area. In BFRC3(0), the evident disorder distribution of basalt fibers was observed, and the large agglomeration of basalt fibers increased the possibility of defects. A large number of basalt fibers passed through the pores and ITZ area, denoting its importance in cracking resistance and toughening. However, the content of hydration products at the interface is low (which is related to the decrease of cementitious materials per unit volume caused by the increase of the content of basalt fibers), the basalt fibers cannot be fully wrapped, and larger pores can be observed. According to the above analysis, it can be concluded that the proper

incorporation of basalt fiber is beneficial to the improvement of mechanical properties and durability of concrete, and the microstructure of initial hydration product interface of each group of concrete is consistent with its initial macro-mechanical properties index.

After 20 cycles of salt-freezing–drying–wetting (Fig. 9), the obvious point-like and short columnar gypsum crystals were observed at the interface of hydration products of concrete in each group. This is because at low temperature, the TSA-type destruction (Musa & Yang, 2006) is the major type of sulfate erosion, and the main erosion product is the expansive gypsum crystal. Under the action of frost heaving force and expansion stress, the pores on the interface of hydration products of concrete begin to increase, and the pores of group C are the obviously presented. Basalt fiber reinforced concrete has the phenomenon of increasing pores and porosity, but we could see the partition in the fiber through pores, bridging, basalt fiber formation of the three-dimensional network and good elastic modulus part. It can be made to slow down the freeze pressure (Powers, 1954) and capillary osmosis (Powers & Helmuth, 1953) the expansion

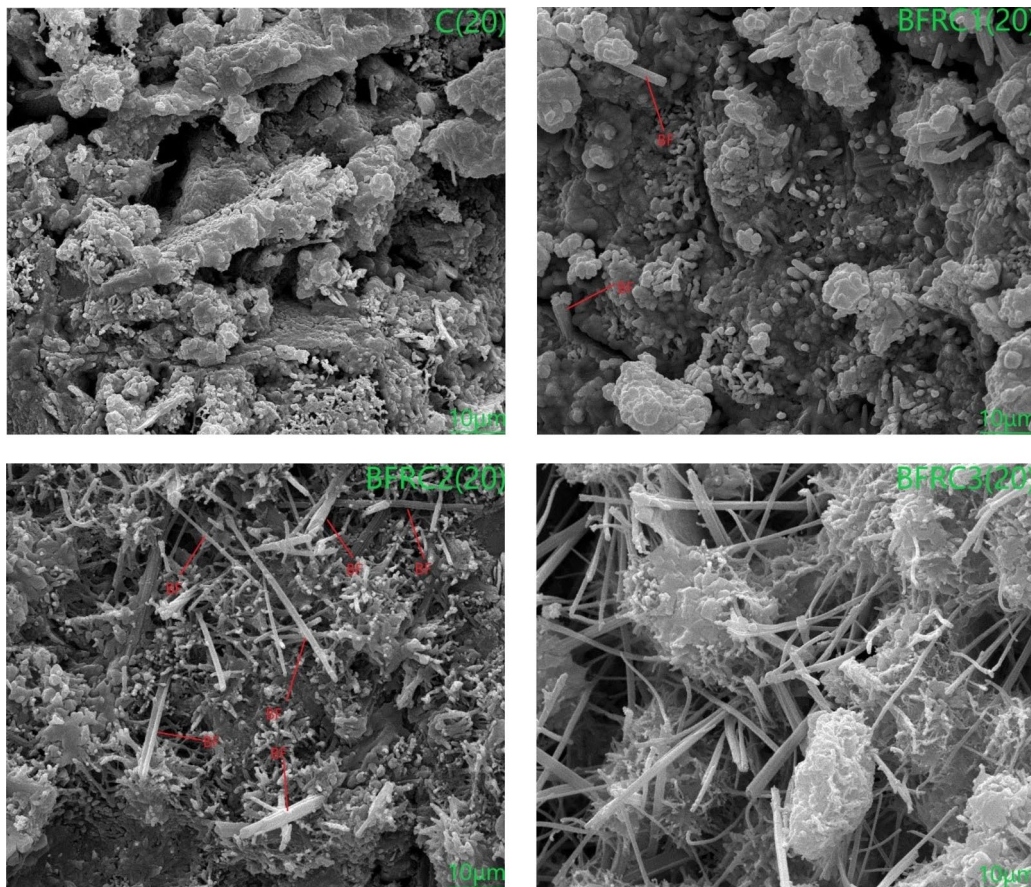


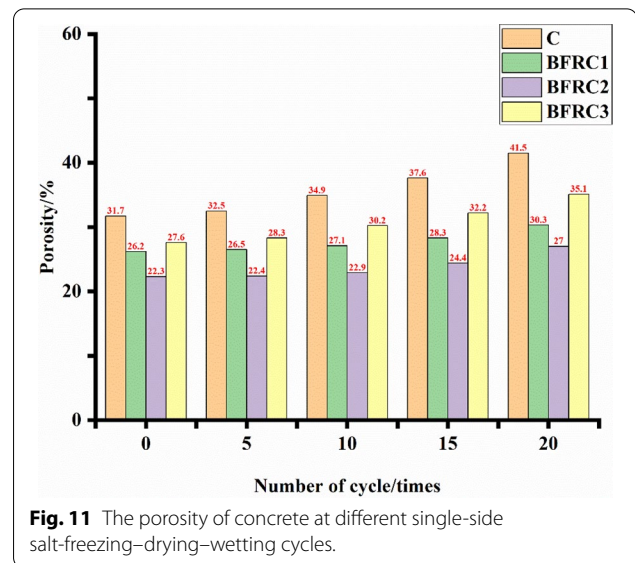
**Fig. 9** The SEM of concrete subjected to 20 times of single-side salt-freezing–drying–wetting cycles.

stress of tensile stress, sulfate crystallization. BFRC2 group has the highest compactness and integrity. Due to the small amount of basalt fiber in BFRC1 group, basalt fiber in pores and cracks become less, in which case basalt fiber cannot exert the partition and bridge function. In BFRC3 group, a large amount of basalt fibers can be observed exposed at interface. Lacking of adequate hydration products with coordination, there are a lot of basalt fibers between the pores. Despite that the framework of the basalt fiber network is obvious, the compactness and integrity of it are still poor. On comparing the initial state with three groups of basalt fiber reinforced concrete interface we observed, the basalt fiber surface parcel of hydration products marginally reduce [TSA damage will cause C–S–H gel decomposition (Liu et al., 2015)], basalt fibers and bondability of hydration products began to reduce, more directly exposed in the interface of basalt fiber.

After 20 times of single-side salt-freezing–drying–wetting cycles (Fig. 10), we can observe basalt fibers with a little micro-cracks and crystal surface, but the overall form is still intact, indicating that single-side salt-freezing–drying–wetting cycle has less effect on the basalt fibers, thus, basalt fibers in this kind of work environment can still keep the excellent toughness and crack resistance performance.

### 3.3 Pore Structure

MIP test was used to study the influence of different cycles on the pore structure of concrete in single-side salt-freezing–drying–wetting cycle. The research on pore structure mainly focuses on porosity (Fig. 11), pore size distribution (Figs. 12, 13, 14, 15) and critical pore size (Fig. 16). Porosity is closely related to the compressive strength of concrete, the lower the



porosity of concrete, the denser the structure, the higher of the compressive strength; pore size distribution and critical pore size are closely related to concrete permeability and durability. It can be implied from Fig. 11 that the addition of basalt fiber will reduce the original porosity of concrete, which is consistent with the studies of some scholars (Jiao et al., 2019). However, it was found that the BFRC2 group had the lowest original porosity, and that of BFRC3 group was higher than that of BFRC1 and BFRC2 groups, which was related to excessive fiber incorporation and large amount of fiber disordered agglomeration, increasing the possibility of defects. The porosity of concrete in each group began to increase with the development of single-side salt-freezing–drying–wetting cycle. The tensile stress

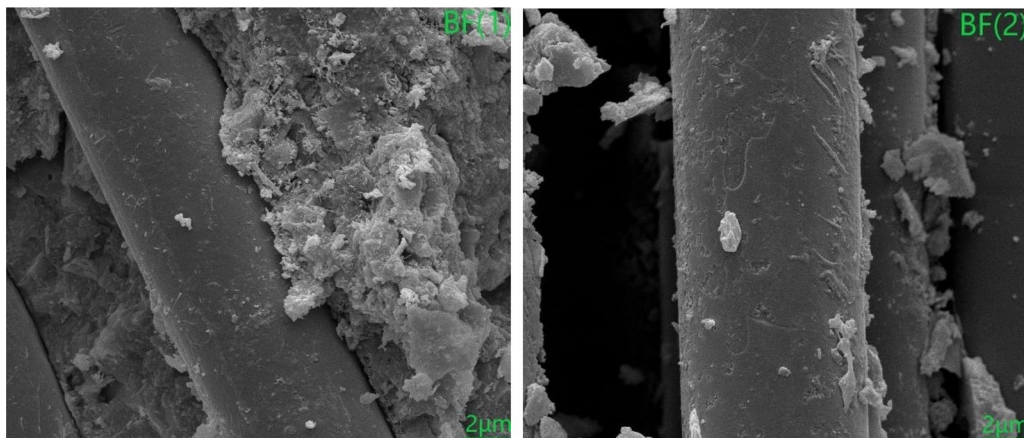


**Fig. 10** The SEM of basalt fiber subjected to 20 times of single-side salt-freezing–drying–wetting cycles.

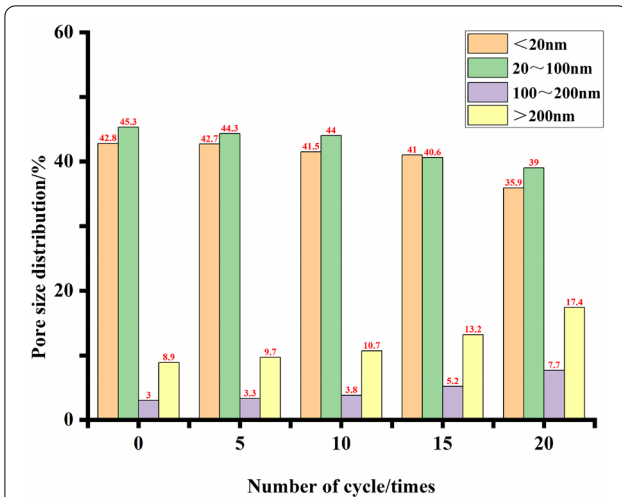


**Fig. 12** The pore size distribution of concrete at different single-side salt-freezing-drying-wetting cycles (C).

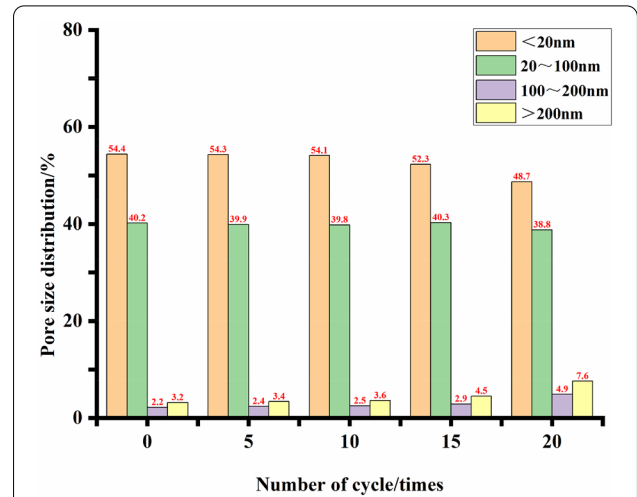


**Fig. 14** The pore size distribution of concrete at different single-side salt-freezing-drying-wetting cycles (BFRC2).

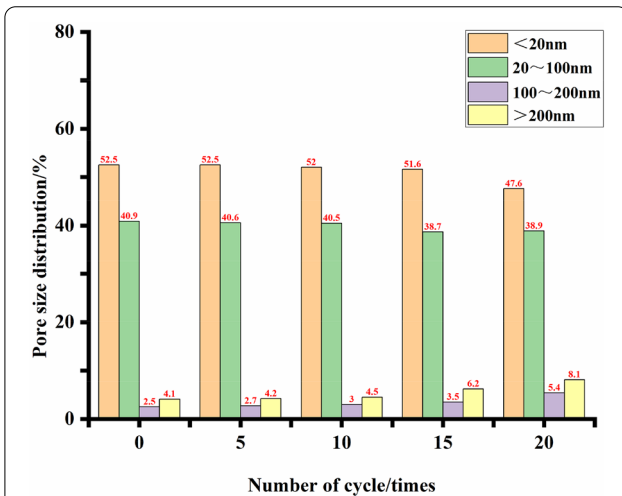


**Fig. 13** The pore size distribution of concrete at different single-side salt-freezing-drying-wetting cycles (BFRC1).

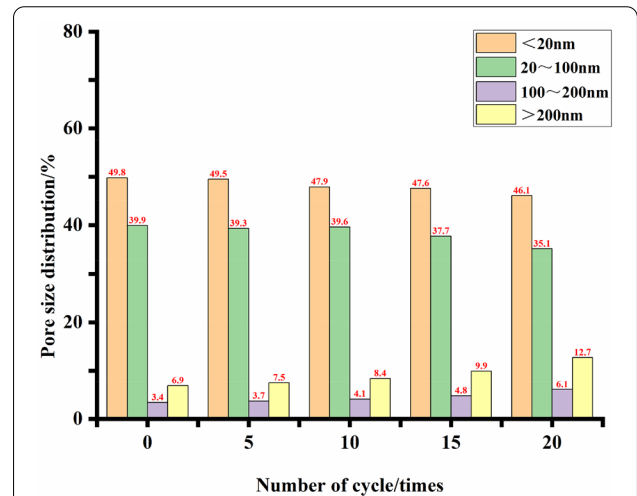
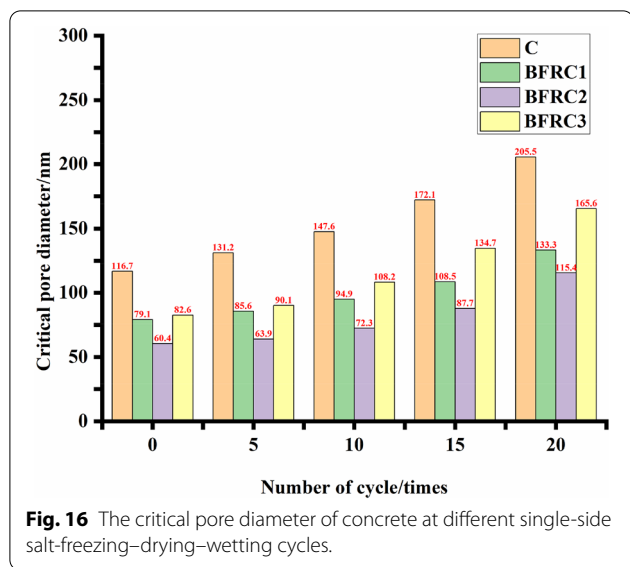


**Fig. 15** The pore size distribution of concrete at different single-side salt-freezing-drying-wetting cycles (BFRC3).

caused by freezing pressure (Powers, 1954) and capillary osmotic pressure (Powers & Helmut, 1953), along with the expansion stress caused by sulfate crystallization, increased the porosity of concrete. After 20 cycles, the porosity of concrete in group C, BFRC1, BFRC2 and BFRC3 increased by 9.8%, 4.1%, 4.7% and 7.5%, respectively. It can be seen that the addition of basalt fiber reduces the increase of concrete porosity under single-side salt-freezing-drying-wetting cycle. That is because, on the one hand, the incorporation of basalt fiber improves the compactness of concrete, improves the content and depth of concrete resistance to sulfate ion erosion; on the other hand, the toughness and crack

resistance of basalt fiber reduces the stress concentration and the damage caused by it.

Some scholars (Wu, 1979) divided the pores into harmless pore (<20 nm), less harmful pore (20–100 nm), harmful pore (100–200 nm) and multi-harmful pore (>200 nm) in accordance with the pore size. In the initial state, the pore size of concrete is mainly concentrated in the two ranges of harmless pore and less harmful pore. The total proportion of harmless pore and less harmful pore in group C, BFRC1, BFRC2 and BFRC3 were 88.1%, 93.4%, 94.6% and 89.7%, respectively (Figs. 12, 13, 14, 15). The increase of small pores will exert a positive effect on the compressive strength



of concrete. Because large pores affect the fluidity of concrete, basalt fiber is difficult to function as the way it should be. The percentages of harmful pore and multi-harmful pore in group C, BFRC1, BFRC2 and BFRC3 were 3.0%, 2.5%, 2.2% and 3.4%, respectively. The percentages of harmful pore in group C, BFRC1, BFRC2 and BFRC3 were 8.9%, 4.1%, 3.2% and 6.9%, respectively. The addition of basalt fiber reduces the proportion of more damage pore and less damage pore of concrete and effectively improves the durability of concrete. With the advance of single-side salt-freezing-drying-wetting cycle, the concrete pore diameter gradually becomes larger, and the proportion of harmful pore and multi-harmful pore begin to increase. On the one hand, the increase of the proportion of harmful pore and multi-harmful pore accelerates the invasion of sulfate ions, and the erosion content and depth begin to increase. On the other hand, more unfrozen water moves to the frozen region and transforms itself into ice crystals, increasing the frost heaving force. After 20 cycles, the percentages of harmful pores in group C, BFRC1, BFRC2 and BFRC3 increased by 4.7%, 2.9%, 2.7% and 2.7%, respectively, while the percentages of multi-harmful pores in group C, BFRC1, BFRC2 and BFRC3 increased by 8.5%, 4%, 3.4% and 5.8%, respectively. The increase of harmful pores and multi-harmful pores directly reduce the durability of concrete. Basalt fiber mixed with effective in reducing the concrete under the environment of single-side salt-freezing-drying-wetting cycle aperture coarsening, the increase of harmful pores and multi-harmful pores were decreased significantly than those of normal concrete (the effect on multi-harmful pore is more obvious). Hence, it is

beneficial to improve the concrete under the environment of single-side salt-freezing-drying-wetting cycle durability performance.

The pore in concrete is a connected and randomly distributed pore structure system. The critical pore diameter (Fig. 16) is the largest pore diameter to connect the larger pores, which can reflect the connectivity of pores. The physical meaning is: if the pore diameter is greater than the critical aperture, it cannot be connected to each other; if the pore diameter is equal to or less than the critical aperture, it can be connected other pores. Therefore, in cement-based material pore structure system, the smaller the critical pore size, the better the impermeability and durability. The critical pore diameter of concrete in each group under different cycles is shown in Fig. 16. Under 0 cycles, the critical pore diameter of group C, BFRC1, BFRC2 and BFRC3 are 116.7 nm, 79.1 nm, 60.4 nm and 82.6 nm, respectively. The addition of basalt fiber effectively reduces the critical pore diameter of concrete. As the cycle went on, the critical pore size of concrete in each group increased continuously. After 20 cycles, the critical pore sizes of group C, BFRC1, BFRC2 and BFRC3 were 205.5 nm, 133.3 nm, 115.4 nm and 165.6 nm, respectively. The increase of critical pore size weakens the permeability resistance of concrete, which is not conducive to the stability of concrete in service under the condition of single-side salt-freezing-drying-wetting cycle. The growth rate of each major cycle of concrete in group C increased steadily. The growth rate of concrete in group BFRC1 and BFRC2 increased significantly after 10 cycles, while that in group BFRC3 increased significantly after 5 cycles. It is shown that although basalt fiber has the effect of toughening and cracking resistance, it still needs the synergistic effect of cementing material and appropriate amount of basalt fiber for the best effect. In each cycle, the critical pore diameter corresponding to impermeability and durability of concrete is consistent with its macroscopic performance index.

### 3.4 Relationship Between Pore Structure and Mechanical Properties

Figs. 17 and 18 demonstrate the relationship between porosity and mechanical properties of concrete. With the increase of porosity, groups of concrete compressive strength, splitting tensile strength decreases, indicating that under the single-side salt-freezing-drying-wetting cycle concrete porosity and the concrete compressive strength, splitting tensile strength has certain relevance. The correlation coefficients between porosity and compressive strength and splitting tensile strength of concrete in group C, BFRC1, BFRC2 and BFRC3 are all above 0.9, indicating that the correlation

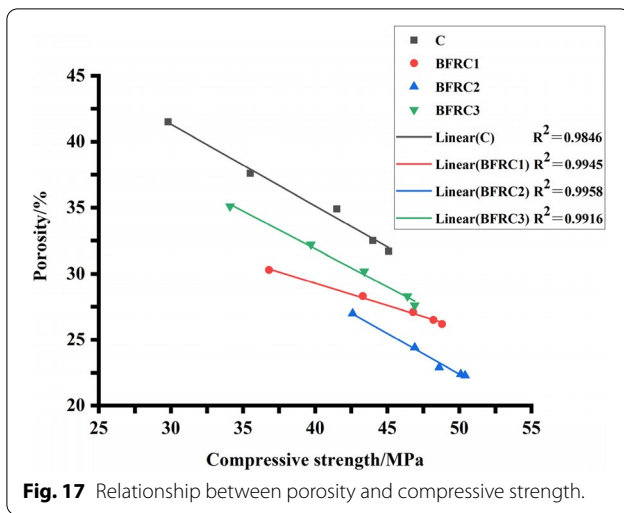


**Fig. 17** Relationship between porosity and compressive strength.

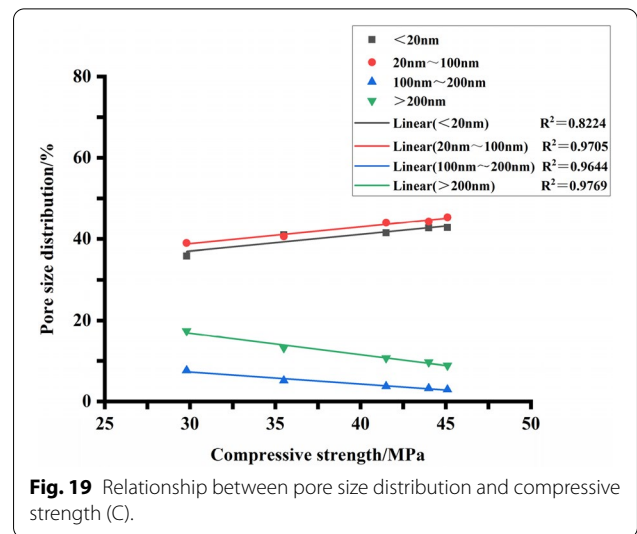


**Fig. 19** Relationship between pore size distribution and compressive strength (C).

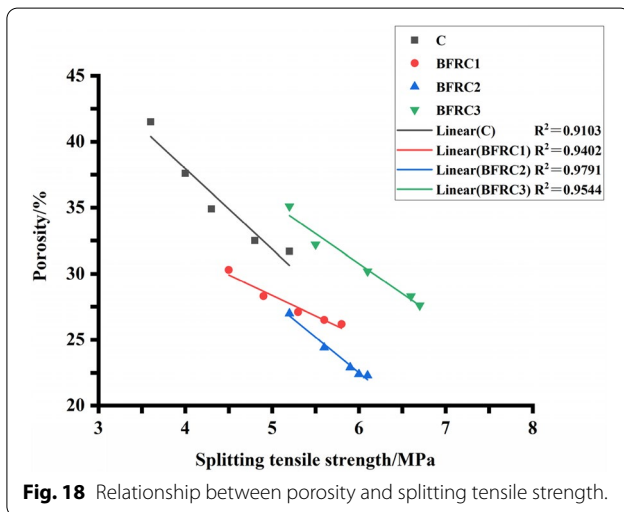


**Fig. 18** Relationship between porosity and splitting tensile strength.

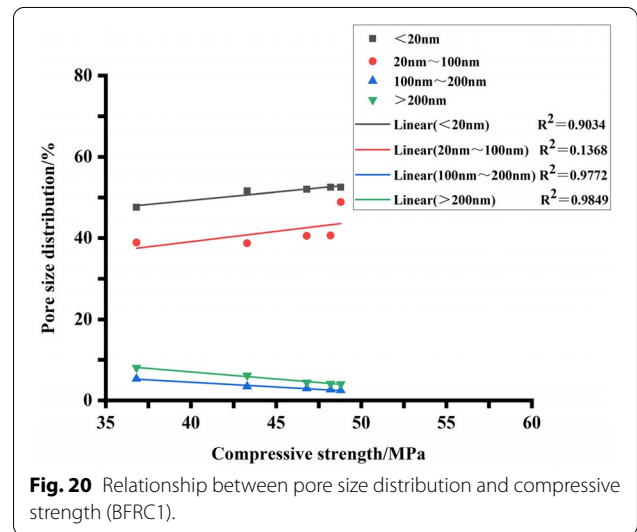
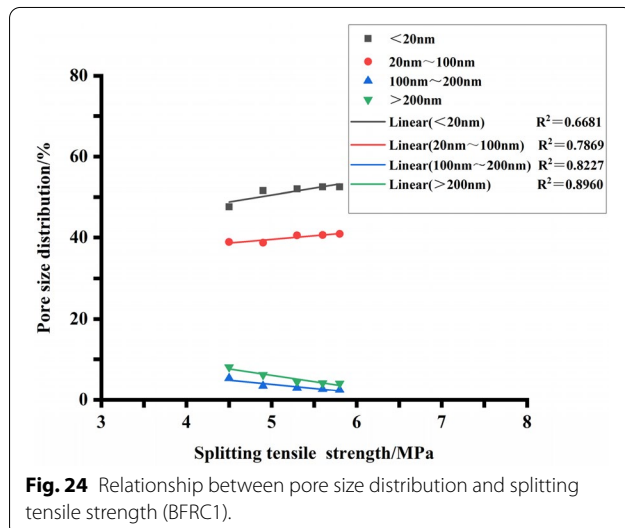
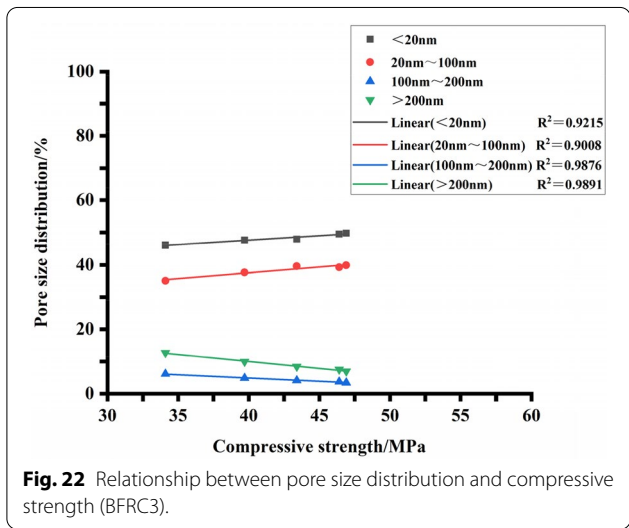
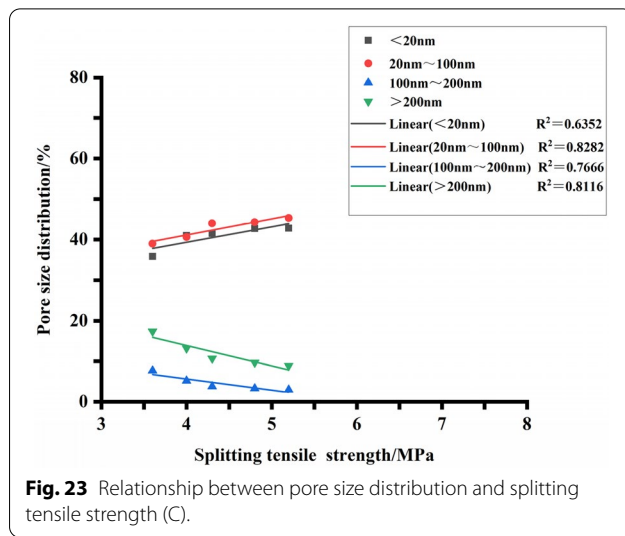
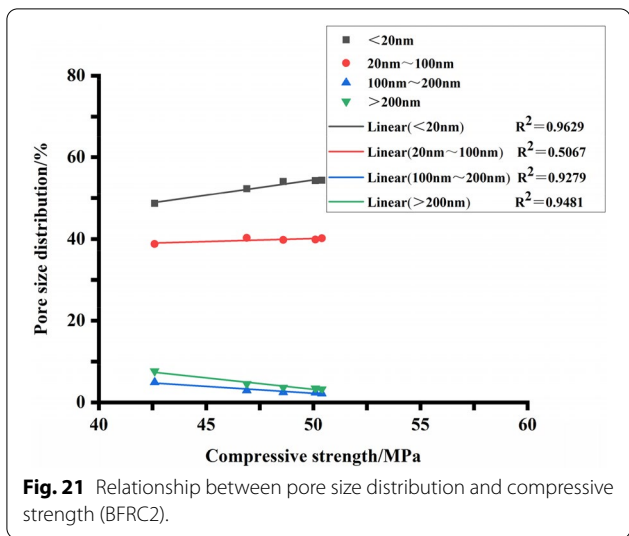


**Fig. 20** Relationship between pore size distribution and compressive strength (BFR1).

between porosity and compressive strength and splitting tensile strength is significant. The correlation coefficient between porosity and splitting tensile strength of concrete in each group is lower than that between porosity and compressive strength, indicating that the influence of porosity on splitting tensile strength of concrete is slightly lower than that of compressive strength under single-side salt-freezing–drying–wetting cycle. In terms of pore size distribution (Figs. 19, 20, 21, 22, 23, 24, 25, 26), the compressive strength and splitting tensile strength of concrete in each group increase with the increase of harmless pores and less harmful pores, while the compressive strength and splitting tensile strength decrease with the increase of harmful pores and multi-harmful pores, which is consistent with the findings of previous studies. The pore size range with the highest correlation of the

compressive strength of concrete in each group is multi-harmful pore (>200 nm), which also indicates that multi-harmful pore has the greatest influence on the compressive strength of concrete. The pore size range of C, BFR1, BFR2 and BFR3 concrete with the highest correlation of splitting tensile strength is 20–100 nm, >200 nm, <20 nm and <20 nm, respectively, displaying a disorder state, which may be related to the three-dimensional network constructed by basalt fiber, however, the specific reasons need further study. The correlation coefficients between critical pore diameter and compressive strength and splitting tensile strength of concrete in group C, BFR1, BFR2 and BFR3 are all above 0.9 (Figs. 27, 28), indicating that



the correlation between critical size diameter and compressive strength and splitting tensile strength is also very significant.

### 4 Conclusion

- (1) Single-side salt-freezing–drying–wetting cycle has obvious damage effect on concrete. The addition of basalt fiber can effectively delay and alleviate the deterioration of mechanical properties of concrete. The positive effect is most obvious when the basalt fiber is 0.2 Vol%, the compressive strength loss rate of basalt fiber concrete is 45.7% and tensile strength loss rate is 48.1% of ordinary concrete after 20 times

- under single-side salt-freezing–drying–wetting cycles.
- (2) Single-side salt-freezing–drying–wetting cycle may cause decomposition and destruction of concrete hydration products, the influence of gelled material and the synergy of basalt fiber. However, it has little influence on basalt fiber and its constructed three-dimensional network, and the positive effect of basalt fiber on the splitting tensile strength of concrete is less affected than that of compressive strength in the same environment.
- (3) The addition of basalt fiber would reduce the porosity and critical pore size of concrete, and change the pore size distribution of concrete: the number of harmless and less harmful pores will increase, and

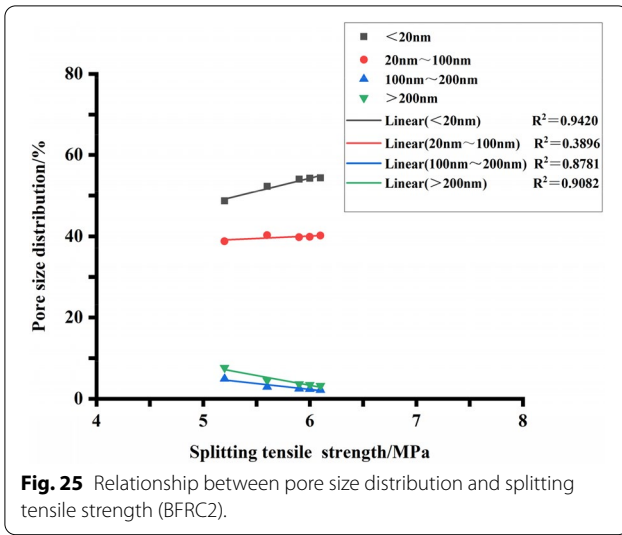


**Fig. 25** Relationship between pore size distribution and splitting tensile strength (BFRC2).

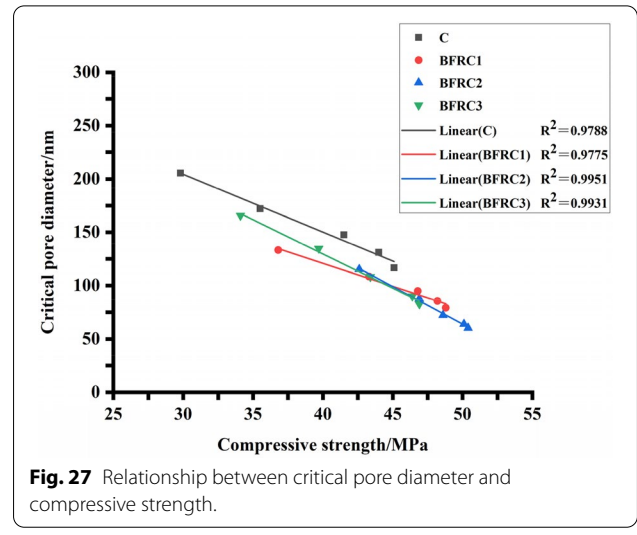


**Fig. 27** Relationship between critical pore diameter and compressive strength.

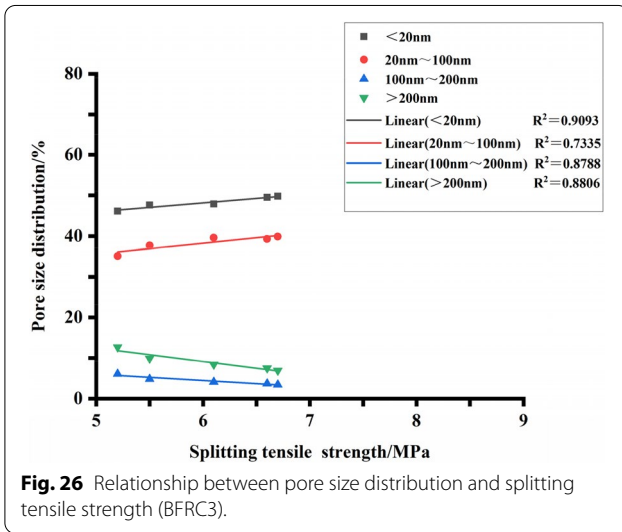


**Fig. 26** Relationship between pore size distribution and splitting tensile strength (BFRC3).

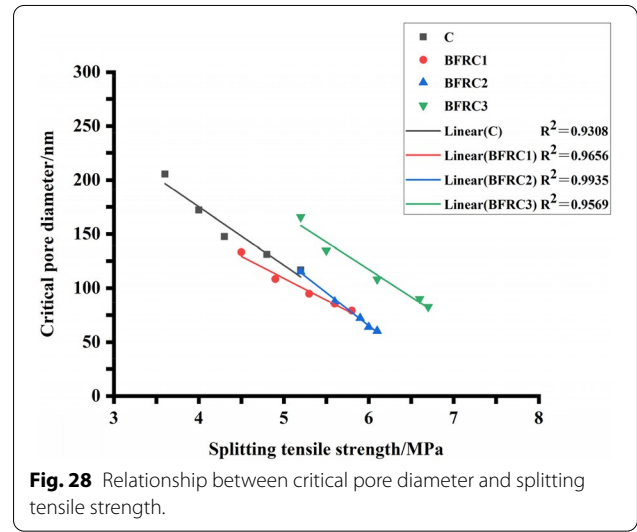


**Fig. 28** Relationship between critical pore diameter and splitting tensile strength.

the number of harmful and multi-harmful pores will decrease. The addition has positive effect on mechanical properties and durability of concrete, which is most obvious when the basalt fiber volume content is 0.2%, however, too much basalt fiber will weaken the positive effect, even bring reverse effects.

- (4) Single-side salt-freezing–drying–wetting cycle can result in the coarsening of concrete pore size diameter. The addition of basalt fiber can effectively reduce the coarsening of concrete pore size diameter under the single-side salt-freezing–drying–wetting cycle, and the effect on multi-harmful pores is most evident.

- (5) The porosity and critical pore size of concrete have strong correlation with compressive strength and splitting tensile strength under the single-side salt-freezing–drying–wetting cycle. The pore size diameter with the highest correlation between the compressive strength of ordinary concrete and basalt fiber reinforced concrete is multi-harmful pore (>200 nm). The pore sizes of ordinary concrete, 0.1 vol% basalt fiber reinforced concrete, 0.2 vol% basalt fiber reinforced concrete and 0.3 vol% basalt fiber reinforced concrete with the highest correlation of split tensile strength are 20–100 nm, >200 nm, <20 nm and <20 nm, respectively, showing a disorder state. This may be related to the three-dimen-

sional network constructed by basalt fiber, whereas the specific reasons need to be further studied.

#### Author contributions

HZ: program design, data analysis, experimental operation, paper writing. JZ: funding management, data calculation, paper revision. YL: funding management, paper revision. XS: data analysis. CZG: experimental operation. KZ: experimental operation. All authors read and approved the final manuscript.

#### Authors' information

Hao Zeng, master student, Department of Architectural Engineering, School of Civil, Architectural and Environmental Engineering, Hubei University of Technology, 28 Nanli Road, Wuhan 430068, Hubei Province, People's Republic of China. Jin Zhang, assistant professor, Department of Architectural Engineering, School of Civil, Architectural and Environmental Engineering, Hubei University of Technology, 28 Nanli Road, Wuhan 430068, Hubei Province, People's Republic of China. Yang Li, professor, Department of Architectural Engineering, School of Civil, Architectural and Environmental Engineering, Hubei University of Technology, 28 Nanli Road, Wuhan 430068, Hubei Province, People's Republic of China. Xin Su, master student, Department of Architectural Engineering, School of Civil Engineering, Guangzhou University, 230 Huanxi Road, Guangzhou 510006, Guangdong Province, People's Republic of China. CongZhi Gu, master student, Department of Architectural Engineering, School of Civil, Architectural and Environmental Engineering, Hubei University of Technology, 28 Nanli Road, Wuhan 430068, Hubei Province, People's Republic of China. Kai Zhang, master student, Department of Architectural Engineering, School of Civil, Architectural and Environmental Engineering, Hubei University of Technology, 28 Nanli Road, Wuhan 430068, Hubei Province, People's Republic of China.

#### Funding

This research was financially supported by the National Nature Science Foundation of China (No. 51508171), Natural Science Foundation of Hubei Province (No. 2020CFB860), Open Foundation of Bridge Safety Monitoring Technology and Equipment Engineering Technology Research Center of Hubei Province (No. QLZX2014001), High Level Talent Foundation of Hubei University of Technology (No. BSQD13042).

#### Availability of data and materials

All data and materials involved in the manuscript are available.

#### Declarations

#### Ethics approval and consent to participate

The content involved in this manuscript meets the academic ethics.

#### Consent for publication

We have carefully read the publication notes and agree to publish.

#### Competing interests

The authors declare that they have no competing interests.

#### Author details

<sup>1</sup>School of Civil, Architectural and Environmental Engineering, Hubei University of Technology, Wuhan 430068, China. <sup>2</sup>School of Civil Engineering, Guangzhou University, Guangzhou 510006, China. <sup>3</sup>Department of Architectural Engineering, School of Civil, Architectural and Environmental Engineering, Hubei University of Technology, 28 Nanli Road, Wuhan 430068, People's Republic of China.

Received: 2 November 2021 Accepted: 21 May 2022

Published online: 16 August 2022

#### References

- Afrouhsabet, V., & Ozbakkaloglu, T. (2015). Mechanical and durability properties of high-strength concrete containing steel and polypropylene. *Construction and Building Materials*, *94*(30), 73–82.
- Afroz, M., Patnaikuni, I., & Venkatesan, S. (2017). Chemical durability and performance of modified basalt fiber in concrete medium. *Construction and Building Materials*, *154*, 191–203.
- Aybu, T., Shafiq, N., & Nuruddin, M. F. (2014). Mechanical properties of high-performance concrete reinforced with basalt fibers. *Procedia Engineering*, *77*, 131–139.
- Bassuoni, M. T., & Nehdi, M. L. (2009). Durability of self-consolidating concrete to sulfate attack under combined cyclic environments and flexural loading. *Cement and Concrete Research*, *39*(3), 206–226.
- Bernard, E. S. (2015). Age-dependent changes in post-crack performance of fiber reinforced shotcrete linings. *Tunnelling and under-Ground Space Technology*, *49*, 241–248.
- Branston, J., Das, S., Kenno, S. Y., & Taylor, C. (2016). Mechanical behaviour of basalt fibre reinforced concrete. *Construction and Building Materials*, *124*(OCT.15), 878–886.
- Dhand, V., Mittal, G., Rhee, K. Y., Park, S. J., & Hui, D. (2015). A short review on basalt fiber reinforced polymer composites. *Composites Part B: Engineering*, *73*, 166–180.
- Dias, D. P., & Thaumaturgo, C. (2005). Fracture toughness of geopolymeric concretes reinforced with basalt fibers. *Cement and Concrete Composites*, *27*, 49–54.
- Dong, J. F., Wang, Q. Y., & Guan, Z. W. (2017). Materials properties of basalt fiber reinforced concrete made with recycled earthquake waste. *Construction and Building Materials*, *130*, 241–251.
- Elmahay, A., & Verleysen, P. (2019). Tensile behavior of woven basalt fiber reinforced composites at high strain rates. *Polymer Testing*, *76*, 207–221.
- Flore, V., Scalici, T., Di Bella, G., & Valenza, A. (2015). A review on basalt fibre and its composites. *Composites, Part B: Engineering*, *74*, 74–94.
- Gao, J. M., Yu, X. X., & Song, L. G. (2013). Durability of concrete exposed to sulfate attack under flexural loading and drying-wetting cycles. *Construction and Building Materials*, *39*(2), 33–38.
- Gzigany, T., Poloskei, K., & Karger-Kocsis, J. (2005). Fracture and failure behavior of basalt fiber mat-reinforced vinyl ester/epoxy hybrid resins as a function of resin composition and fiber surface treatment. *Journal of Materials Science*, *33*(2), 133.
- High, C., Seliem, H. M., El-Safty, A., & Rizkalla, S. H. (2015). Use of basalt fibers for concrete structures. *Construction and Building Materials*, *96*, 37–46.
- Huang, Q., Shi, X. S., Wang, Q. Y., Tang, L., & Zhang, H. E. (2015). The influence of fiber on the resistance to chloride-ion penetration of concrete under the environment of carbonation. *International conference on materials science and applications* (pp. 223–228). Atlantis Press.
- Jiao, H., Han, Z., Chen, X., Yang, Y., & Wang, Y. (2019). Flexural toughness evolution of basalt fiber reinforced shotcrete based on NMR technology. *Journal of China Coal Society*, *44*(10), 2990–2998.
- Kayali, O., Haque, M. N., & Zho, B. (2003). Some characteristics of high strength fiber reinforced lightweight aggregate concrete. *Cement and Concrete Composites*, *25*(2), 207–213.
- Khaled, M., Erenb, Z., & Brahim, Y. (2011). Compression specific toughness of normal strength steel fiber reinforced concrete (NSSFRC) and high strength steel fiber reinforced concrete (HSSFRC). *Materials Research*, *14*(2), 239–247.
- Khan, M., Cao, M., & Ali, M. (2018). Effect of basalt fibers on mechanical properties of calcium carbonate whisker-steel fiber reinforced concrete. *Construction and Building Materials*, *192*, 742–753.
- Khooshechin, M., & Tanzadeh, J. (2018). Experimental and mechanical performance of shotcrete made with nanomaterials and fiber reinforcement. *Construction and Building Materials*, *165*, 199–205.
- Kizilkanat, A. B., Kabay, N., Akyüncü, V., Chowdhury, S., & Akça, A. H. (2015). Mechanical properties and fracture behavior of basalt and glass fiber reinforced concrete: An experimental study. *Construction and Building Materials*, *100*, 218–224.
- Krasnovskikh, M. P., Maksimovich, N. G., Vaisman, Y. I., & Ketov, A. A. (2014). Thermal stability of mineral-wool heat-insulating materials. *Russian Journal of Applied Chemistry*, *87*(10), 1430–1434.
- Kuder, K. G., & Shah, S. (2010). Processing of high-performance fiber-reinforced cement based composites. *Construction and Building Materials*, *24*(2), 181–186.

- Lau, A., & Anson, M. (2006). Effect of high temperature on high performance steel fiber reinforced concrete. *Cement and Concrete Research*, 36(9), 1698–1707.
- Lee, J. J., Song, J., & Kim, H. (2014). Chemical stability of basalt fiber in alkaline solution. *Fibers and Polymers*, 15(11), 2329–2334.
- Li, W., & Wu, J. (2009). Mechanical properties of basalt fiber reinforced geopolymeric concrete under impact loading. *Materials Science and Engineering A*, 505(1–2), 178–186.
- Liu, K., Deng, M., Mo, L., & Tang, J. (2015). Deterioration mechanism of Portland cement paste subjected to sodium sulfate attack. *Advances in Cement Research*, 27(8), 477–486.
- Lu, L. L., Wei, J., & Bi, Q. W. (2017). Salt corrosion resistance of basalt fiber reinforced concrete in early age. *Journal of Dalian Jiaotong University*, 32(5), 178–183. in Chinese.
- Ludovico, M. D., Prota, A., & Manfredi, G. (2012). Structural upgrade using basalt fibers for concrete confinement. *Journal of Composites for Construction*, 14(5), 541–552.
- Monaldo, E., Nerilli, F., & Vairo, G. (2019). Basalt-based fiber-reinforced materials and structural applications in civil engineering. *Composite Structures*, 214, 246–263.
- Musa, M., & Yang, Z. (2006). The factors affecting concrete durability and its prevention and control measures are brief discuss. *Westren Exploration Project*, 18(12), 249–250. in Chinese.
- Ollivier, J. P., Maso, J. C., & Bourdette, B. (1995). Interfacial transition zone in concrete. *Advanced Cement Based Materials*, 2(1), 30.
- Powers, T. C. (1954). Void spacing as a basis for producing air-entrained concrete. *ACI Journal*, 50(9), 741.
- Powers, T. C., & Helmuth, R. A. (1953). Theory of volume changes in hardened Portland cement paste during freezing. *Proceedings Highway Research Board*, 32, 285.
- Rashiddadash, P., Ramezaniapour, A. A., & Mahdikhani, M. (2014). Experimental investigation on flexural toughness of hybrid fiber reinforced concrete (HFRC) containing metakaolin and pumice. *Construction and Building Materials*, 51, 313–320.
- Ren, W. B., Xu, J. Y., & Su, H. Y. (2016). Dynamic compressive behavior of basalt fiber reinforced concrete after exposure to elevated temperatures. *Fire and Materials*, 40(5), 738–755.
- Sadrromtazi, A., Tahmouresi, B., & Saradar, A. (2018). Effect of silica fume on mechanical strength and microstructure of basalt fiber reinforced cementitious composites (BFRCC). *Construction and Building Materials*, 162, 321–333.
- Sahmaran, M., Erdem, T. K., & Yaman, I. O. (2007). Sulfate resistance of plain and blended cements exposed to wetting-drying and heating-cooling environments. *Construction and Building Materials*, 21(8), 1771–1778.
- Shengji, J., Zhongliang, L., Jian, Z., & Yanling, W. (2015). Experimental study on anti-freezing and thawing performance of reinforced concrete of basalt fiber under corrosion condition. *Engineering Mechanics*, 32(5), 178–183.
- Sim, J., & Park, C. (2005). Characteristics of basalt fiber as a strength. *Composites Part B: Engineering*, 36, 504–512.
- Sim, J., Park, C., & Moon, D. Y. (2005). Characteristics of basalt fiber as a strengthening material for concrete structures. *Composites, Part B: Engineering*, 36(6/7), 504–512.
- Sukontasukkul, P., Pomchiengpin, W., & Songpiriyakij, S. (2010). Post-crack flexural response and toughness of fiber-reinforced concrete after high temperature exposure. *Construction and Building Materials*, 24(10), 1967–1974.
- Taha, A., Alnahhal, W., & Alnuaimi, N. (2020). Bond durability of basalt FRP bar to fiber reinforced concrete in saline environment. *Composite Structures*, 243, 112277.
- Wang, D., Wang, L., Gu, X., & Zhou, G. (2013). Effect of basalt fiber on the asphalt binder and mastic at low temperature. *Journal of Materials in Civil Engineering*, 25(3), 355–364.
- Wu, Z. W. (1979). Discussion on the recent development direction of concrete science and technology. *Journal of the Chinese Ceramic Society*, 3, 262–270. in Chinese.
- Yang, L., Yao, Z., Xue, W., Wang, X., Kong, W., & Wu, T. (2019). Preparation, performance test and microanalysis of hybrid fibers and microexpansive high-performance shaft lining concrete. *Construction and Building Materials*, 223, 431–440.
- Yao, Z., Li, X., Wu, T., Yang, L., & Liu, X. (2019). Hybrid-fiber-reinforced concrete used in frozen shaft lining structure in coal mines. *Materials*, 12(23), 3988.
- Yew, M. K., Mahmud, H. B., Shafiq, P., Ang, B. C., & Yew, M. C. (2015). Effects of poly propylene twisted bundle fibers on the mechanical properties of high-strength oil palm shell lightweight concrete. *Materials and Structures*, 49(4), 1221–1233.
- Zeynep, A., & Mustafa, O. (2018). The properties of chopped basalt fibre reinforced self-compacting concrete. *Construction and Building Materials*, 186, 678–685.
- Zhang, H., Wang, B., Xie, A. Y., & Qi, Y. (2017). Experimental study on dynamic mechanical properties and constitutive model of basalt fiber reinforced concrete. *Construction and Building Materials*, 152, 154–167.
- Zhao, Y. R., Wang, L., Lei, Z. K., Han, X. F., & Shi, J. N. (2018). Study on bending damage and failure of basalt fiber reinforced concrete under freeze-thaw cycles. *Construction and Building Materials*, 163, 460–470.

## Publisher's Note

Springer Nature remains neutral with regard to jurisdictional claims in published maps and institutional affiliations.

Submit your manuscript to a SpringerOpen<sup>®</sup> journal and benefit from:

- Convenient online submission
- Rigorous peer review
- Open access: articles freely available online
- High visibility within the field
- Retaining the copyright to your article

Submit your next manuscript at ► [springeropen.com](https://www.springeropen.com)